JCTC Journal of Chemical Theory and Computation

Article

pubs.acs.org/JCTC

Toward the Understanding of the Photophysics and Photochemistry of 1-Nitronaphthalene under Solar Radiation: The First Theoretical Evidence of a Photodegradation Intramolecular Rearrangement Mechanism Involving the Triplet States

Angelo Giussani*

Instituto de Ciencia Molecular, Universitat de València, Apartado22085, ES-46071 Valencia, Spain

Supporting Information

ABSTRACT: 1-Nitronaphthalene belongs to the class of nitrated polycyclic aromatic hydrocarbons, and constitutes an atmospheric pollutant commonly found in urban environments due to its production during incomplete combustions. On the basis of CASPT2//CASSCF quantum chemical calculations, the photophysics and photochemistry of the system under solar exposure have for the first time been studied. According to the characteristics of the incident radiation (either UVA or UVB, both present in the portion of the solar spectrum reaching the earth), a different excited state will be mainly populated. In both cases, the main decay path undertaken by the corresponding bright state leads to an efficient intersystem crossing process toward the $^3(\pi_O\pi^*)$ triplet excited state. The population of the triplet manifold is then identified as the primary photoinduced process in the title molecule, not only after UVA interaction but also under UVB exposure. From the $^3(\pi_O\pi^*)$ state, the system can either decay in a radiationless manner to the original ground state minimum, or undergo a photodegradation process mediated by the presence of an accessible singlet−triplet crossing region characterized by the formation of a oxaziridine ring. The determination of such a photodegradation path constitutes the first theoretical evidence supporting the hypothesis formulated almost 50 years ago in the seminal work of Chapman et al. (*J. Am. Chem. Soc.* **1966**, *88*, 5550), according to which the photolysis undertaken by nitrated polycyclic aromatic hydrocarbons proceeds through an intramolecular rearrangement mechanism, here characterized on the triplet manifold.

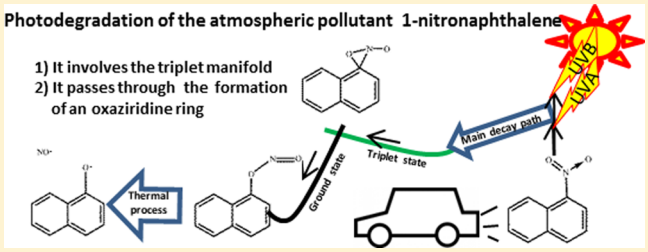

INTRODUCTION

Nitrated polycyclic aromatic hydrocarbons (NPAHs) are a vast group of molecules comprising more than two hundred different compounds. Most of them cause potentially dangerous effects on both human health and ecosystems.[1] For example, 2-nitrofluorene, a common NPAH present in the environment,[2] has been found to be mutagen[3] and carcinogen[4] to animals. Since NPAHs are mainly produced during incomplete combustions, a process that normally occurs in most of the vehicles,[5] they constitute a considerable class of pollutants in urban atmosphere.

The interaction of UV radiation with NPAHs can lead to their photodegradation into nitrogen(II) oxide (NO·) plus the corresponding aryloxy radical (Ar−O·) and, consequently, represents a way of removal of such substances. The degradation process might also cause the formation of new molecules, as the secondary organic aerosol.[6] The mechanistic key elements driving the photodegradation of NPAHs were first addressed in 1966 by Chapman et al., who in particular studied the photochemistry of 9-nitroanthracene.[7] It was concluded that the photoactivated part of the global photodegradation process determines the transformation of the original nitro group into a nitrite group (see Scheme 1), which will subsequently evolve toward the final products of the photodegradation by thermal activation.

Chapman et al. supposed two possible ways leading to such a photoinduced chemical change: a dissociation−recombination process and an intramolecular rearrangement mechanism. The first mechanism is characterized by the cleavage of the CN bond

Scheme 1. Photoactivated Part of the Global Photodegradation Process Undertaken by Nitrated Polycyclic Aromatic Hydrocarbons and the Hypothesized Mechanisms: (a) Dissociation−Recombination Mechanism; (b) Intramolecular Rearrangement Mechanism

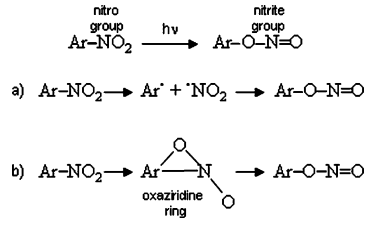

Received: May 6, 2014
Published: July 25, 2014

and a subsequent reaction between the two resulting radicals to form the nitrite compound. The second possibility entails the formation of an oxaziridine ring that will finally evolve into a nitrite group. In the paper, the intramolecular rearrangement mechanism is claimed as the most plausible, since secondary products that will be expected if a dissociation-recombination mechanism will take place, such as anthracene, were not isolated. After the seminal work of Chapman, other studies have confirmed the photodegradation of NPAHs into an aryoxyl radical and nitrogen(II) oxide.[8−10]

One of the most abundant NPAH found in the gas phase is 1-nitronaphthalene, 1NN (see Figure 1). It is characterized by a

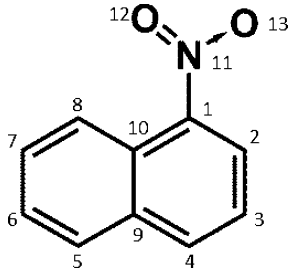

Figure 1. 1-Nitronaphthalene (1NN) structure and atom labeling.

large triplet quantum yield (0.63 ± 0.10);[11] it constitutes the organic compound with the fastest multiplicity change ever measured (around 100 fs);[12−15] it exhibits direct photolysis in gas phase.[16] As other NPAHs, 1NN was considered non-fluorescent, a fact disclaimed by the work of Peon and co-workers, who were able to measure its fluorescence emission in methanol using femtosecond frequency up-conversion techniques.[12]

Different theoretical and experimental efforts have been devoted to the elucidation of the photophysics and photochemistry of 1NN. In 2003, Arey and co-workers determined the rate constants for the photolysis of 1NN under UVA and solar exposure, concluding that gas-phase photodegradation is expected to be the dominant atmospheric loss process for the title molecule.[16] Between 2007 and 2009 the group headed by Professor Peon extensively studied the photophysics and photochemistry of 1NN in methanol and other solvents.[12−14] First, employing femtosecond fluorescence up-conversion techniques, it was determined that the primary photoinduced process undertaken by the $S_1(\pi\pi^*)$ state is an ultrafast decay toward the triplet manifold.[12,13] Then, in 2009, performing a subpicosecond transient absorption study, it was shown the implication of an intermediate triplet T_n state having a partial $n\pi^*$ character in the mechanism experimented by the $S_1(\pi\pi^*)$ in order to decay to the T_1 state.[14] According to the authors, the decay to the T_n state constitutes the actual ultrafast process; meanwhile, the subsequent population of the T_1 state will occur on picosecond time-scale. In the same year, Crespo-Hernández and co-workers confirmed such a result on the basis of broadband transient absorption data recorded in different solutions.[17] A second decay channel connecting the $S_1(\pi\pi^*)$ to a dark dissociative singlet state was also supposed, which was considered partially responsible for the photodegradation of the system. In 2013, Crespo-Hernández and co-workers further characterized the excited state dynamic of 1NN, performing a series of studies on 1NN, 2-nitronaphthalene, and 2-methyl-1-nitronaphthalene.[18−20] The inverse relation experimentally detected between the magnitude of the photodegradation and triplet quantum yield for the mentioned molecules was taken as an evidence of the implication in the photodegradation process of a dark singlet excited state. It was then concluded that after excitation, the 1NN $S_1(\pi\pi^*)$ state can undergo two different ultrafast decay processes. One will lead to the population of a $T_n(n\pi^*)$ state, as previously shown by the works of Peon and co-workers.[12−14] The other will determine the population of a dark singlet excited state having intramolecular charge-transfer character $S_{dis}(CT)$. Such state was claimed to be the responsible for the photodissociation mechanism of 1NN into the corresponding aryloxy radical and nitrogen(II) oxide, through a dissociation-recombination mechanism (see Scheme 1b). Most of the presented works were supported by the computation of theoretical calculations at the DFT level. In 2012, Canuto and co-workers studied the system employing ab initio methods and, in particular, the CASPT2//CASSCF protocol.[21] It was found that the $S_1(\pi\pi^*)$ and the $T_2(n\pi^*)$ states become progressively degenerate along the evolution experimented by the former state from the Franck−Condon region. Due to the high spin−orbit coupling (SOC) computed between such states, it was concluded that the described conditions characterizing the $S_1(\pi\pi^*)$ decay path entail the intrinsic molecular reasons leading to the ultrafast intersystem crossing process experimentally detected for the 1NN molecule.

As far as the author known, a theoretical ab initio study on the photophysics and photochemistry of the title molecule under UVA and UVB radiation has not been performed. In fact, in the paper published by Canuto and co-workers, it is described only the decay from the $S_1(\pi\pi^*)$ excited state, without considering the population of higher excited states under UVA and UVB exposure. Since the exploration of such a possibility would account for the photoresponse of the system under solar radiation, it will be of fundamental importance in order to determine the photophysics and photochemistry of such an atmospheric pollutant.

Different questions still remain open regarding the photodegradation mechanism. It is not clear if the process occurs in the singlet and/or in the triplet manifold. Despite the hypothesis formulated by Crespo-Hernández and co-workers,[18,19] according to which a dark singlet excited state plays the main role in the photodegradation reaction, it is significant to notice that for other NAPHs the triplet excited states have been instead claimed to be involved.[7,22,23] Recently, it was found by Crespo-Hernández and co-workers that the presence of molecular oxygen reduces the photodegradation quantum yield of 1NN by 63%, a fact that points out the importance of the triplet states for the photodegradation process.[20] Even more unclear remains the relative importance of the dissociation-recombination mechanism and of the intramolecular rearrangement mechanism for the photodissociation of 1NN.

In order to describe the main decay paths undertaken by the system under solar radiation, and with the aim of providing new insights on the photodegradation mechanism, in the present contribution the photophysics and photochemistry of 1NN after UVA and UVB exposure have been studied using the CASPT2//CASSCF protocol and following the principles of the so-called "photochemical reaction path approach".[24]

■ COMPUTATIONAL DETAILS

The present study has been performed by using the well-tested CASPT2//CASSCF methodology[25−27] as implemented in the MOLCAS 7.4 software.[28] Optimized structures and minimum energy paths (MEPs) have been then calculated at the

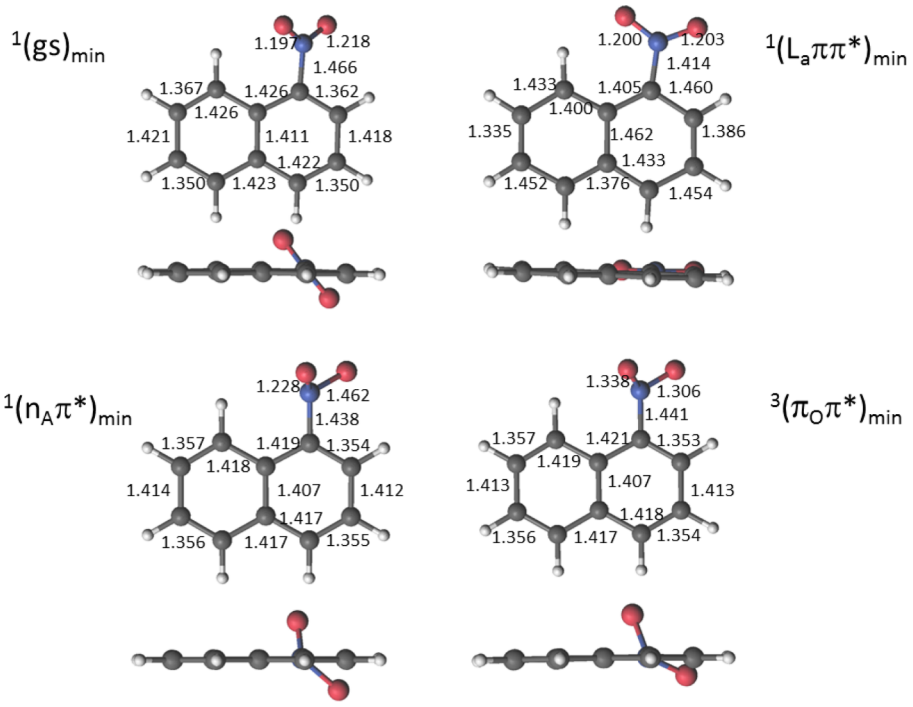

Figure 2. Frontal and side views of 1-nitronaphthalene CASSCF minima structures including selected bond lengths (in Ångstrom).

multiconfigurational CASSCF level, and at the geometries so obtained, the dynamic correlation effects have been taken into account by performing second-order multiconfigurational CASPT2 calculations. No restrictions to the symmetry of the molecule have been imposed (C_1 symmetry). The basis set of atomic natural orbital (ANO) of L-type contracted to C,N [4s,3p,1d]/H[2s1p] has been employed.[29,30] An active space composed of 16 active electrons distributed in 13 active orbitals has been used in all the final vertical calculations [CASSCF-(16,13)]. As shown in Figure S1 of the Supporting Information (SI), the selected active space takes into account both the π nature of the system and the lone pairs of the oxygen atoms. Due to the computational effort associated with such an extended active space, a reduced number of active electrons and orbitals has been used in the optimization procedures. In particular, for the characterization of $\pi\pi^*$ states, the six active orbitals depicted in Figure S2 of the Supporting Information, and the corresponding six active electrons, have been included in the active space [CASSCF(6,6)]. For the optimization of nπ^* states, the active space of six electrons distributed among six orbitals reported in Figure S3 of the Supporting Information has been employed [CASSCF(6,6)]. Such a strategy was proved successful for different systems,[31] and it was actually used in a recent paper on the photophysics and photochemistry of 1NN.[21]

Within the CASPT2 calculations, an imaginary level-shift correction of 0.2 au has been used in order to minimize the effects of possible intruder states. The CASPT2 standard zeroth-order Hamiltonian has been used as originally implemented.[26] The core orbitals have been frozen in the CASPT2 calculations. Such CASPT2 approach has been validated during the last decades in many different studies on organic molecules, providing a correct prediction, description, and interpretation of photophysical experimental data.[32−35] The research of the evolution of the excited states has been performed by means of MEP calculations,[36,37] using mass-weighted coordinates. This technique provides the steepest descendent path, in which each step is built by the minimization of the energy on a hyperspherical cross section of the potential energy hypersurface centered on the initial geometry within a predefined radius. The importance and reliability of results obtained using such a computational tool have been proven in many different studies, which confirms MEP calculations as a valuable procedure for the description of the photophysics and photochemistry of a molecule.[38,39] In order to connect some important regions of the potential energy hypersurface, linear interpolation of internal coordinate (LIIC) calculations have been performed.[40] Conical intersections and singlet−triplet crossing regions not obtained along MEP calculations have been computed by using the restricted Lagrange multipliers technique as included in the MOLCAS 7.4 package, in which the lowest-energy point is obtained under the restriction of degeneracy between the two considered states.[28] In the regions of the potential energy hypersurfaces where two or more states of different spin multiplicity are degenerate, the corresponding SOC have been calculated, as described elsewhere.[41]

RESULTS AND DISCUSSION

Franck−Condon Geometry. The optimization of the ground state has led to the nonplanar equilibrium geometry reported in Figure 2, hereafter denoted as $^1(gs)_{min}$. The values of the dihedral angles between the atoms $C_{10}C_1N_{11}O_{12}$ and $C_2C_1N_{11}O_{13}$, which can be used in order to evaluate the position of the oxygen atoms with respect to the plane of the naphthalene ring, are in fact equal to −50.87° and −49.68, respectively (see Table 1). The nonplanarity of the ground state equilibrium structure is in agreement with previous studies, and it was justified by the presence of the *peri* H atom, whose is expected to force the distribution of torsion angles away from 0°.[18,19,21]

At the Franck−Condon geometry, four singlet and five triplet excited states have been calculated and analyzed. The lowest singlet excited state, S_1, is characterized by a CASSCF wave

dx.doi.org/10.1021/ct500395f | J. Chem. Theory Comput. 2014, 10, 3987−3995

Table 1. Important Geometrical Parameters Characterizing the Position of the Nitro Group with Respect the Naphthalene Ring for Different Optimized Structures: the Dihedral Angle Defined by the $C_{10}C_1N_{11}O_{12}$ Atoms; the Dihedral Angle Defined by the $C_2C_1N_{11}O_{13}$ Atoms; the Angle Between the $O_{12}N_{11}O_{13}$ Positions; and the Angle Among the $C_{10}C_1N_{11}$ Atoms[a]

structure	$C_{10}C_1N_{11}O_{12}$	$C_2C_1N_{11}O_{13}$	$O_{12}N_{11}O_{13}$	$C_{10}C_1N_{11}$
$^1(gs)_{min}$	−50.87	−49.68	125.00	120.14
$^1(L_a\pi\pi^*)_{min}$	0.97	0.84	122.51	123.99
$^1(n_A\pi^*)_{min}$	−84.80	−40.36	112.00	117.64
$^3(\pi_O\pi^*)_{min}$	−71.32	−25.16	111.22	118.00
$(^1n_A\pi^*/^3\pi_O\pi^*)_{STC}$	−48.70	−48.34	123.79	123.22
$(^3\pi_O\pi^*/gs)_{STC}$	−91.09	−23.76	97.40	117.65

[a]All the reported values are expressed in degrees.

Table 2. Calculated Vertical Excitation Energies at the Franck−Condon Geometry (E_{VA}, eV) for the Lowest Valence Singlet and Spin Forbidden Triplet Excited States[a]

state	E_{VA} (eV)	f	μ (D)
S_0 gs	0.00		4.06
T_1 $^3(\pi\pi^*)$	3.03		3.99
T_2 $^3(n_A\pi^*)$	3.66		2.92
T_3 $^3(\pi_O\pi^*)$	3.67		2.60
S_1 $^1(n_A\pi^*)$	3.88	0.00347	2.71
S_2 $^1(L_b\pi\pi^*)$	3.89	0.00117	3.69
T_4 $^3(\pi\pi^*)$	3.90		3.97
S_3 $^1(n_B\pi^*)$	4.14	0.00073	3.20
T_5 $^3(n_B\pi^*)$	4.31		3.02
S_4 $^1(L_a\pi\pi^*)$	4.38	0.05538	8.67

[a]The computed dipole moments (μ, D) and the oscillator strengths (f) for the singlet−singlet transitions are also included.

function in which the main contribution is given by the configuration state function associated with a one-electron promotion from the H − 7 orbital to L orbital (see SI Figure S4). The H − 7 orbital can be regarded as describing the lone pairs of the oxygen atoms in an antibonding orientation, while the L orbital has mainly π character. Consequently, the state will be referred as $^1(n_A\pi^*)$. The CASSCF wave function of the second lowest singlet excited state is mainly composed by the minus linear combination of the H − 6 → L (28%) and H−1 → L + 2 (20%) configurations. Due to the close resemblance observe between such configuration state functions and the ones characterizing the state classified, according to Platt nomenclature, as the $^1(L_b\pi\pi^*)$ for the naphthalene system (see SI Figure S5 and S9), the S_2 state can be coined as the $^1(L_b\pi\pi^*)$. The S_3 state again describes an excitation involving the oxygen lone pairs, here displaying a bonding orientation (see SI Figure S6), and it will be named $^1(n_B\pi^*)$. Finally, the highest calculated singlet excited wave function represents a $^1(L_a\pi\pi^*)$ state, as can be deduced by the comparison with the homonymous state for the naphthalene system (see SI Figure S7 and S10).

A similar analysis has been also performed for the calculated triplet excited states. It has been obtained that the T_1 and T_4 states display $\pi\pi^*$ nature, while the T_2 and the T_5 states can be classified as the $^3(n_A\pi^*)$ and the $^3(n_B\pi^*)$ states, respectively. The T_3 state is characterized by a CASSCF wave function composed by a configuration state function describing a $\pi \rightarrow \pi^*$ one electron promotion that involves orbitals mainly localized on the nitro group (see SI Figure S8). Accordingly, the T_3 will be hereafter named $^3(\pi_O\pi^*)$.

For the sake of clarity, in Tables S1 and S2 of the Supporting Information are reported for each state the configurations that contribute to the corresponding CASSCF wave function with a weight greater or equal to 10%.

The obtained results are in agreement with the work of Canuto and co-workers,[21] according to which the S_1 state is the $^1(n_A\pi^*)$, T_1 has $\pi\pi^*$ nature, and the T_2 state is the $^3(\pi_O\pi^*)$. The latter has been here described as the T_3 state, although taking into account the precision of the employed method, it can actually be considered degenerate with the T_2 (see Table 2).

Main Decay Paths. According to the computed values of the oscillator strengths and of the vertical excitation energies (see Table 2), it is possible to assume that after UVA absorption (3.10−3.94 eV) the system will be mainly describe in the $^1(n_A\pi^*)$ state, while the interaction with UVB radiation (3.94−4.43 eV) will primarily cause the population of the $^1(L_a\pi\pi^*)$ state. Both UVA and UVB wavelengths, although in different percentage, are present in the spectra of radiation found in the environment. Consequently, in order to account for the photophysics and photochemistry of 1NN under solar radiation (which is particularly interesting since the molecule constitutes an atmospheric pollutant), the evolution of the system from the Franck−Condon geometry on the $^1(L_a\pi\pi^*)$ and the $^1(n_A\pi^*)$ states has been studied.

As shown by the computation of the corresponding MEP calculation at the CASPT2//CASSCF level (see Figure 3a), the $^1(L_a\pi\pi^*)$ state can decay from the Franck−Condon region toward a minimum structure, hereafter denoted as $^1(L_a\pi\pi^*)_{min}$. Along such MEP, the system undergoes two main geometrical deformations. First, the single−double bond character of the carbon−carbon bonds is interchanged with respect to the ground state minimum (see Figure 2). Second, according to the values of the $C_{10}C_1N_{11}O_{12}$ and $C_2C_1N_{11}O_{13}$ dihedral angles (see Table 1), the nitro group appears in the plane of the naphthalene ring, which consequently determines the global planarity of the $^1(L_a\pi\pi^*)_{min}$ structure.

At the $^1(L_a\pi\pi^*)_{min}$ structure, the $^1(L_a\pi\pi^*)$ state is almost degenerate with the $^1(n_A\pi^*)$ and the $^3(\pi_O\pi^*)$ states, which are both placed at 4.06 eV above the ground-state minimum (see Table 3). Such a situation will allow the population of the $^1(n_A\pi^*)$ state through an internal conversion process, which can further decay to the $^3(\pi_O\pi^*)$ potential energy hypersurface by means of an intersystem crossing mechanism. In fact, at the $^1(L_a\pi\pi^*)_{min}$ region the $^1(n_A\pi^*)$ and $^3(\pi_O\pi^*)$ states are strongly coupled, as proven by the computed high value of the related SOC (70.18 cm^{-1}).

From the $^1(L_a\pi\pi^*)_{min}$ minimum, the $^3(\pi_O\pi^*)$ state can undergo the decay described by the corresponding MEP that leads to an equilibrium structure hereafter named $^3(\pi_O\pi^*)_{min}$ (see Figure 3b). At such region, the naphthalene ring has recovered the single−double bond alternation characteristic of the Franck−Condon geometry, while the nitro group presents different important distortions (see Figure 2). The $C_{11}O_{12}$ and the $C_{11}O_{13}$ bonds are elongated by 0.141 and 0.086 Å with respect the ground state minimum, respectively. The sizable difference between the absolute values of the $C_{10}C_1N_{11}O_{12}$ and $C_2C_1N_{11}O_{13}$ dihedral angles (see Table 1) reflects the fact that in the $^3(\pi_O\pi^*)_{min}$ structure the $C_1N_{11}O_{12}O_{13}$ atoms do not stay in the same plane. The O_{12} oxygen is, in fact, much more perpendicular to the plane of the naphthalene ring than the O_{13} atom.

dx.doi.org/10.1021/ct500395f | J. Chem. Theory Comput. 2014, 10, 3987−3995

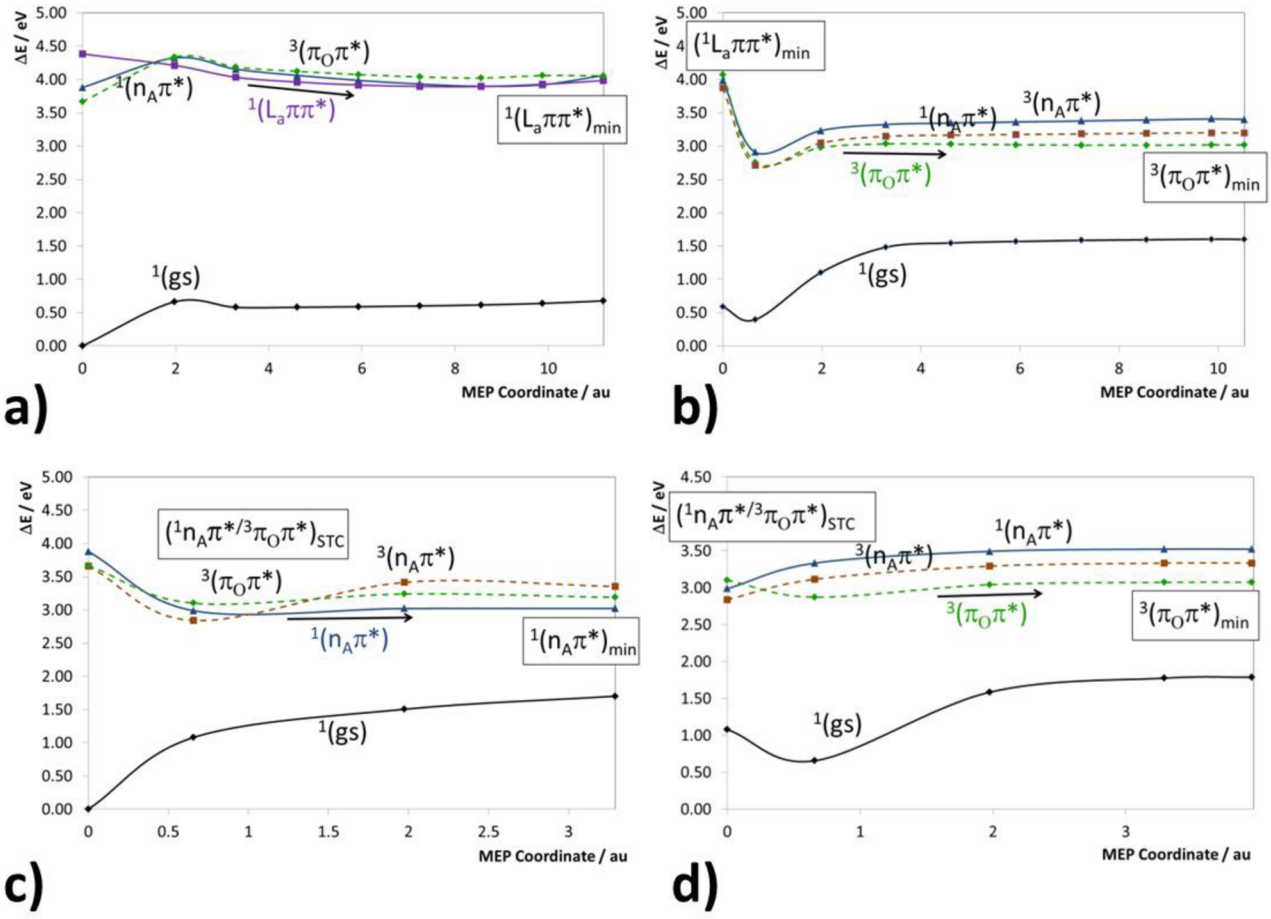

Figure 3. Energy profiles of the ground and the most photophysical and photochemical relevant singlet and triplet excited states of 1-nitronaphthalene along the computed minimum energy path (MEP): (a) MEP on the $^1(L_a\pi\pi^*)$ state from the Franck−Condon geometry; (b) $^3(\pi_O\pi^*)$ MEP from the $^1(L_a\pi\pi^*)_{min}$ minimum; (c) MEP on the $^1(n_A\pi^*)$ state from the Franck−Condon geometry; and (d) $^3(\pi_O\pi^*)$ MEP from the $(^1n_A\pi^*/^3\pi_O\pi^*)_{STC}$ intersystem crossing region. In each graphic, the electronic state whose MEP has been computed is written using the same color associated with its potential energy hypersurface (while the other states are reported in black) and an arrow is drawn nearby the calculated MEP profile.

Table 3. Computed Energies (eV) for the Most Relevant Singlet and Triplet States of 1-Nitronaphthalene at Different Important Geometries[a]

structure	gs	$^1(L_a\pi\pi^*)$	$^1(n_A\pi^*)$	$^3(\pi_O\pi^*)$
$^1(gs)_{min}$	0.00	4.38	3.88	3.67
$^1(L_a\pi\pi^*)_{min}$	0.68	3.99	4.06	4.06
$^1(n_A\pi^*)_{min}$	1.70		3.02	3.19
$^3(\pi_O\pi^*)_{min}$	1.60		3.40	3.02
$(^1n_A\pi^*/^3\pi_O\pi^*)_{STC}$	1.08		2.99	3.10
$(^3\pi_O\pi^*/gs)_{STC}$	3.74			3.73
$(^3\pi_O\pi^*/gs)_{STC\text{-}pd}$	3.71			3.73
$^1(gs)_{nitrite}$	0.32			

[a]All the reported values are referred to the ground state optimized geometry, $^1(gs)_{min}$.

According to the results presented above, the evolution of the system after absorption into the bright $^1(L_a\pi\pi^*)$ state can lead to the population of the $^3(\pi_O\pi^*)_{min}$ minimum region. In the following, it is shown how the same photophysical outcome can be caused by absorption into the bright $^1(n_A\pi^*)$ state.

The evolution of the $^1(n_A\pi^*)$ state from the Franck−Condon region has been characterized by the computation of the corresponding MEP (see Figure 3c), which leads through a barrierless path to an equilibrium structure, named $^1(n_A\pi^*)_{min}$. At the minimum geometry, the molecule presents geometrical distortions similar to the ones observed at the $^3(\pi_O\pi^*)_{min}$ structure. The $N_{11}O_{13}$ bond is particularly elongated, displaying an increasing with respect to the ground state minimum of 0.224 Å. The O_{12} atom is almost perpendicular to the naphthalene ring, as proven by the value of the $C_{10}C_1N_{11}O_{12}$ dihedral angle, which is nearly equal to 90°.

At the $^1(n_A\pi^*)_{min}$ structure, the energy order of the $^1(n_A\pi^*)$ and the $^3(\pi_O\pi^*)$ states is reversed with respect to the one found at the Franck−Condon region (see Tables 2 and 3). Along the obtained MEP on the $^1(n_A\pi^*)$ state a singlet−triplet crossing region has been localized between the $^1(n_A\pi^*)$ and the $^3(\pi_O\pi^*)$ states, hereafter denoted as $(^1n_A\pi^*/^3\pi_O\pi^*)_{STC}$. Being placed in the first part of the MEP, the $(^1n_A\pi^*/^3\pi_O\pi^*)_{STC}$ structure partially resemble the Franck−Condon geometry (see Figure 4). The geometrical parameters characterizing the nitro group and its orientation within the molecule have undergone only minors changings, while the main distortion is localized on the naphthalene ring, which already presents the single−double bond alternation described in the $^1(n_A\pi^*)_{min}$ structure. Due to the degeneracy in energy and the computed high value of the SOC between the $^1(n_A\pi^*)$ and the $^3(\pi_O\pi^*)$ states (66.63 cm^{-1}), it is possible to consider the $(^1n_A\pi^*/^3\pi_O\pi^*)_{STC}$ region as an efficient gate to the triplet manifold. The $^3(\pi_O\pi^*)$ state can subsequently evolve to the same minimum region characterized

dx.doi.org/10.1021/ct500395f | J. Chem. Theory Comput. 2014, 10, 3987−3995

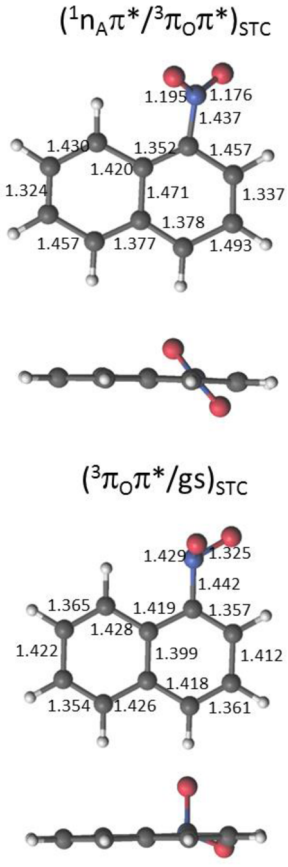

Figure 4. Frontal and side views of 1-nitronaphthalene singlet−triplet crossing regions, including selected bond lengths (in Ångstrom).

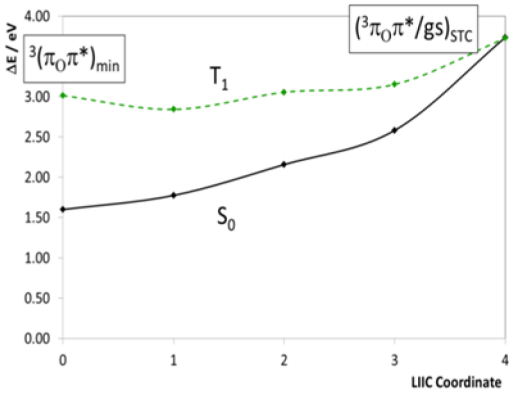

Figure 5. Energy profiles of the ground and lowest triplet excited state of 1-nitronaphthalene along the computed linear interpolation of internal coordinates calculation between the $^3(\pi_O\pi^*)_{min}$ and the $(^3\pi_O\pi^*/gs)_{STC}$ structures.

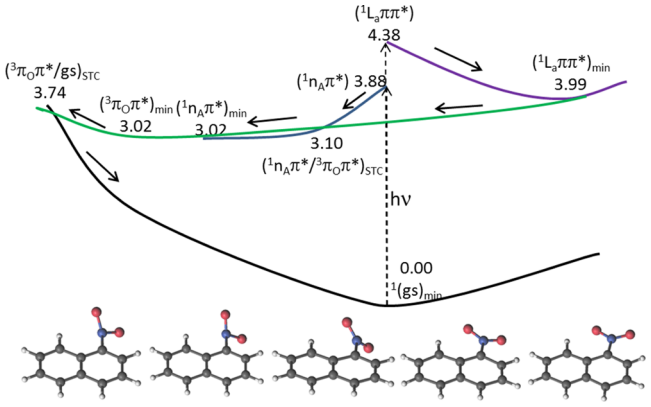

Figure 6. Scheme of the photoinduced processes undertaken by 1-nitronaphthalene after UVA and UVB absorption, resulting in the repopulation of the original ground state. The reported energies (eV) have been calculated at the CASPT2(16,13)//CASSCF(6,6)/ANO-L C,N [4s,3p,1d]/H[2s1p] level of theory.

above, $^3(\pi_O\pi^*)_{min}$, as proven by the computation of the corresponding MEP from the $(^1n_A\pi^*/^3\pi_O\pi^*)_{STC}$ point (see Figure 3d).

From the $^3(\pi_O\pi^*)_{min}$ geometry, the system can further decay surmounting an energy barrier to a nearby singlet−triplet crossing region with the ground state, named as $(^3\pi_O\pi^*/gs)_{STC}$ (see Figure 4). The proximity of such a degenerate point to the region of the potential energy hypersurface, in which the $^3(\pi_O\pi^*)_{min}$ is localized, is reflected by the geometrical resemblance between the two structures. In order to study the potential energy hypersurface connecting the $^3(\pi_O\pi^*)_{min}$ and the $(^3\pi_O\pi^*/gs)_{STC}$, a LIIC calculation have been performed (see Figure 5). According to the results obtained, the system on the $^3(\pi_O\pi^*)$ state will be able to reach the mentioned singlet−triplet crossing region through the surmounting of an energy barrier of the order of the energy difference between the $^3(\pi_O\pi^*)_{min}$ and $(^3\pi_O\pi^*/gs)_{STC}$ structures (around 0.7 eV, see Table 3).

From the $(^3\pi_O\pi^*/gs)_{STC}$ geometry, the system can undergo a relaxation mechanism leading to the original ground state minimum, as the computation of the corresponding MEP has proven, which consequently constitutes a possible nonradiative decay process.

A schematic representation of the described photoinduced processes is presented in Figure 6.

Photodegradation. In the preceding section, it has been shown how both the $^1(L_a\pi\pi^*)$ and the $^1(n_A\pi^*)$ bright states can evolve from the Franck−Condon region to the $^3(\pi_O\pi^*)_{min}$ minimum, from which the system can finally decay through the $(^3\pi_O\pi^*/gs)_{STC}$ singlet−triplet crossing region back to the original ground state geometry. As described in the introduction, 1NN is photodegraded under UV exposure. In agreement with such experimental evidence, besides the nonreactive relaxation mechanism characterized above, it has also been found a photochemical reaction path leading the molecule to the corresponding nitrite compound, whose formation constitutes the photoactivated part of the global photodegradation process.

The key structure here identified as the main gate toward photodegradation is a singlet−triplet crossing region, $(^3\pi_O\pi^*/gs)_{STC\text{-}pd}$, characterized by the chemical recombination of the original nitro group into a oxaziridine ring (see Figure 7). In such geometry, in fact, a new carbon−oxygen bond is formed between the C_1O_{12} atoms, the C_1N_{11} bond is considerably bent out of the naphthalene-ring plane, and the two oxygen atoms are almost perpendicular to each other. At the $(^3\pi_O\pi^*/gs)_{STC\text{-}pd}$ point, the $^3(\pi_O\pi^*)$ and the ground states are almost degenerate (ΔE = 0.02 eV, see Table 3) and present a spin−orbit coupling value of 2.50 cm^{-1}. The latter is considerably smaller than the spin−orbit coupling characterizing the $(^1n_A\pi^*/^3\pi_O\pi^*)_{STC}$ and $^1(L_a\pi\pi^*)_{min}$ regions (66.63 and 70.18 cm^{-1}, respectively), whose particularly high values reflect the property of the system to undergo the fastest multiplicity change ever measured. The $(^3\pi_O\pi^*/gs)_{STC\text{-}pd}$ structure can be reached from the $^3(\pi_O\pi^*)_{min}$ minimum surmounting an energy barrier of at most 0.88 eV, as

dx.doi.org/10.1021/ct500395f | J. Chem. Theory Comput. 2014, 10, 3987−3995

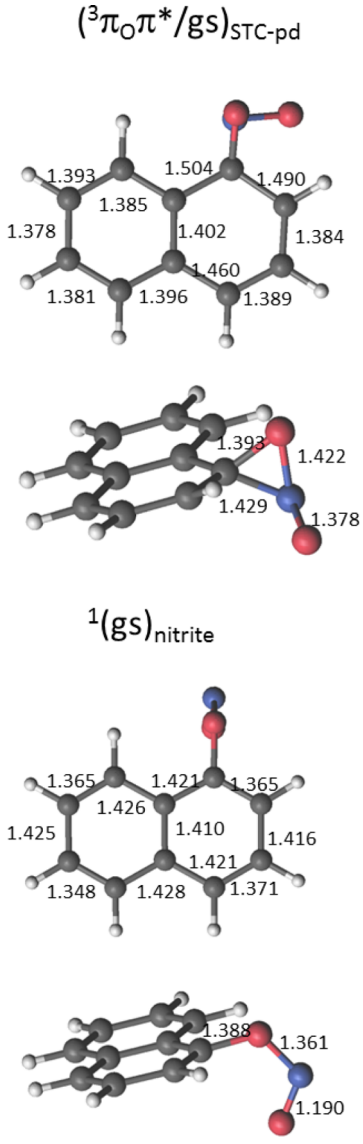

Figure 7. Frontal and side views of 1-nitronaphthalene key structures involved in the photodegradation process, including selected bond lengths (in Ångstrom).

shown by the computation of the corresponding LIIC calculation (see Figure 8).

The relevance of the $(^3\pi_O\pi^*/gs)_{STC\text{-}pd}$ region for the photodegradation process has been studied by the computation of the corresponding MEP on the ground state (see SI Figure S11), which has proven the possibility for the system to decay from the $(^3\pi_O\pi^*/gs)_{STC\text{-}pd}$ geometry toward the related nitrite structure, $^1(gs)_{nitrite}$ (see Figure 7). Finally, the system can dissociate into nitrogen(II) oxide plus the corresponding aryloxy radical undertaking a thermal activated process. A schematic representation of the described photodegradation mechanism is presented in Figure 9.

Discussion. Having described the main results obtained in the present study, it is now important to analyze them in the light of previous theoretical findings and of the available experimental data.[11−21] As pointed out in the introduction, one of the most striking feature of the title molecule is to display the fastest multiplicity change ever measured (around 100 fs). In agreement with the work of Canuto and co-workers,[21] such a behavior can be ascribed to the strong coupling between a $\pi\pi^*$

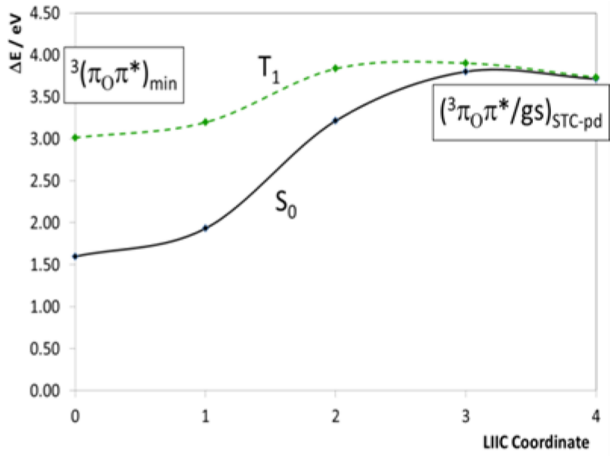

Figure 8. Energy profiles of the ground and lowest triplet excited state of 1-nitronaphthalene along the computed linear interpolation of internal coordinates calculation between the $^3(\pi_O\pi^*)_{min}$ and the $(^3\pi_O\pi^*/gs)_{STC\text{-}pd}$ geometries.

triplet state (here the $^3(\pi_O\pi^*)$) and the lowest singlet excited state (here the $^1(n_A\pi^*)$) that characterized the main decay path experimented by the latter. Moreover, it has been found that also the bright $^1(L_a\pi\pi^*)$ state, populated under UVB exposure, can efficiently decay to the triplet $^3(\pi_O\pi^*)$. The $^1(L_a\pi\pi^*)$ can in fact evolve toward a degenerate region with the $^1(n_A\pi^*)$ state (the $^1(L_a\pi\pi^*)_{min}$ structure), consequently causing the corresponding internal conversion process. Once populated, the $^1(n_A\pi^*)$ state can subsequently decay to the $^3(\pi_O\pi^*)$ state, due to the strong coupling between such states that characterized also the $^1(L_a\pi\pi^*)_{min}$ geometry. The population of the triplet manifold then appears to be the primarily photoinduced process caused by both UVA and UVB exposure.

According to most of the previously published works on the system,[12−21] the triplet state populated by an ultrafast intersystem crossing mechanism from the lowest singlet excited state is the $T_2(n\pi^*)$ state and will subsequently decay to the $T_1(\pi\pi^*)$ in few picoseconds. In agreement with such outcomes, the $^3(\pi_O\pi^*)$ state has here been found as the second lowest triplet excited state in both the characterized regions from which it can be populated (i.e., the $^1(L_a\pi\pi^*)_{min}$ and the $(^1n_A\pi^*/^3\pi_O\pi^*)_{STC}$ structures). Nevertheless, at its corresponding minimum (the $^3(\pi_O\pi^*)_{min}$ geometry), it constitutes the lowest triplet excited state. Consequently, the computed MEP reported in Figure 4d proves that the $^3(\pi_O\pi^*)$ state can decay toward a minimum region where it constitutes the lowest triplet excited state T_1. Due to the presumable crossing between the T_2 and the T_1 along such decay, we cannot, however, exclude the possibility described by Peon and co-workers and Crespo-Hernandez and co-workers of an internal conversion process to a triplet $\pi\pi^*$ state.[20,21] Further studies, probably involving dynamic simulations, are required in order to fully unveil the question.

Regarding the photodegradation mechanism, Crespo-Hernández and co-worker supposed the implication of a dissociative singlet excited state that will evolve toward the photodegradation products through a dissociation-recombination mechanism.[18] In the present work, an intramolecular rearrangement photodegradation mechanism involving the triplet manifold has been instead characterized. The implication of the triplet states in the photodegradation mechanism is supported by the fact that both the brightest singlet excited

dx.doi.org/10.1021/ct500395f | J. Chem. Theory Comput. 2014, 10, 3987−3995

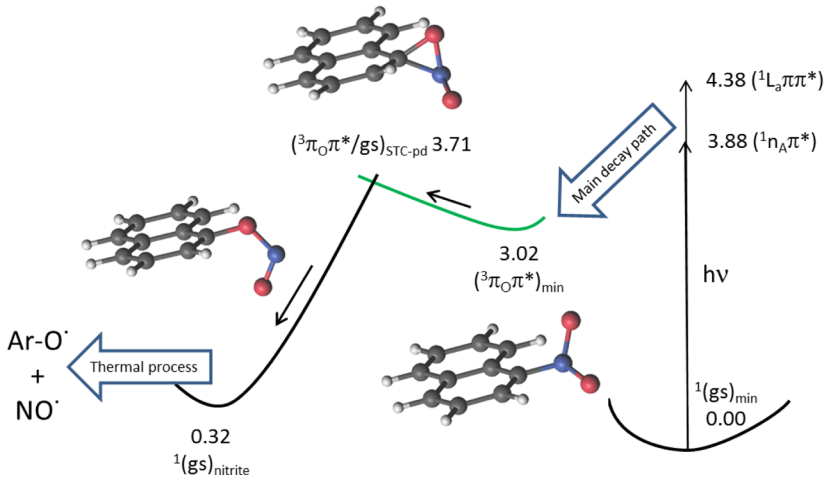

Figure 9. Scheme of the photodegradation intramolecular rearrangement mechanism undertaken by 1-nitronaphthalene after UVA and UVB absorption. The reported energies (eV) have been calculated at the CASPT2(16,13)///CASSCF(6,6)/ANO-L C,N [4s,3p,1d]/H[2s1p] level of theory.

states of the system will mainly decay to the $^3(\pi_O\pi^*)$ state. Moreover, it has been recently reported that the photodegradation quantum yield drastically decreases with the presence of molecular oxygen,[20] pointing out to the likely involvement of the triplet states. Due to the complexity of the system and the intrinsic difficulty of describing photochemical processes, much more work need to be done in order to completely characterize the photodegradation mechanism undertaken by 1NN.

A comment regarding the computed CASPT2//CASSCF MEP is appropriate at this final stage. Analyzing the results reported in Figure 3, it is possible to notice that in some cases the obtained MEP are not strictly barrierless, as it happens, in particular, for the MEP on the $^3(\pi_O\pi^*)$ state from the $^1(L_a\pi\pi^*)_{min}$ geometry. According to the implementation of the MEP technique in the MOLCAS software, a MEP calculation will stop as soon as an increase in the energy of the considered state is registered. The nonbarrierless character of the $^3(\pi_O\pi^*)$ MEP depicted in Figure 3b may consequently reflect a computational inconsistency due to either the reduce active space employed for the MEP calculation, and/or the correction of the CASSCF MEP profiles introduces by the recalculation of the converged points at the CASPT2 level. It is important to highlight that the energy barrier computed along the $^3(\pi_O\pi^*)$ MEP (around 0.25 eV) can still be considered into the error of the method and is still sufficiently low be surmounted. The presence of a small energy barrier along a computed CASPT2//CASSCF MEP has been already reported for other systems.[40,42]

CONCLUSIONS

On the basis of the exploration of the potential energy hypersurfaces of the low-lying singlet and triplet excited states by means of accurate state-of-the-art computational strategies, different important insight on the photophysics and photochemistry of 1-nitronaphthalene have been provided. In particular, the main decay paths of the brightest excited state under UVA and UVB exposure have been characterized computing the corresponding minimum energy paths. According to such an analysis, it has been obtained that form both the $^1(L_a\pi\pi^*)$ and the $^1(n_A\pi^*)$ states an efficiently intersystem crossing mechanism toward the $^3(\pi_O\pi^*)$ state will be expected. The result consequently accounts for the ultrafast multiplicity change (around 100 fs) experimentally observed in the molecule. Once populated, the $^3(\pi_O\pi^*)$ state decays to a minimum structure, from which the system can follow a nonreactive pathway or undertake a photodegradation mechanism. The first possibility is due to the presence of a nearby singlet−triplet crossing region (the $(^3\pi_O\pi^*/gs)_{STC}$ structure) from which the molecule can undergo a nonradiative relaxation process toward the original ground state minimum. The second possibility will lead to the transformation of the nitro substituent into a nitrite group, and it is mediated by the presence of a singlet−triplet crossing region (the $(^3\pi_O\pi^*/gs)_{STC\text{-}pd}$ structure) whose geometry is characterized by the formation of an oxaziridine ring. From the produced nitrite compound, the system will finally split into nitrogen(II) oxide and the corresponding aryloxy radical through a thermal activated process.

The work constitutes the first ab initio exploration of the photophysics and photochemistry of the important atmospheric pollutants 1-nitronaphthalene under solar radiation and provides strong theoretical evidence supporting an intramolecular rearrangement mechanism involving the triplet states for the photodegradation process undertaken by the system.

The present results on 1-nitronaphthalene, together with other studies performed on different naphthalene derivatives,[43] can be used in order to further determine the intrinsic photophysical and photochemical properties of the basic aromatic chromophoric structure composed by the naphthalene ring, as well as the effects produce by the introduction of a particular functional group.

ASSOCIATED CONTENT

Supporting Information

Orbitals used in the active space, main orbitals involved in the different states, minimum energy path calculations, and Cartesian coordinates. This material is available free of charge via the Internet at http://pubs.acs.org.

AUTHOR INFORMATION

Corresponding Author

*Email: Angelo.Giussani@uv.es.

Author Contributions

The manuscript was written through contributions of all authors. All authors have given approval to the final version of the manuscript.

Notes

The authors declare no competing financial interest.

■ ACKNOWLEDGMENTS

This research was supported by the Project CTQ2010-14892 of the Spanish MEC/FEDER and Consolider-Ingenio in Molecular Nanoscience MEC/FEDER CSD2007-0010. A.G. gratefully acknowledges PhD fellowship "V segles" from the Universitat de València.

■ REFERENCES

(1) Möller, L.; Lax, I.; Eriksson, L. C. *Environ. Health Perspect.* **1993**, *101*, 309.
(2) Xu, X.; Nachtman, J.; Rappaport, S.; Wei, E. *J. Appl. Toxicol.* **1981**, *1*, 196.
(3) Wang, Y. I. Y.; Rappaport, S. M.; Sawyer, R. F.; Talcott, R. E.; Wei, E. T. *Cancer Lett.* **1987**, *5*, 39.
(4) Miller, J. A.; Sandin, R. B.; Miller, E. C.; Rush, H. P. *Cancer Res.* **1955**, *15*, 188.
(5) Handa, T.; Yamauchi, T.; Ohnishi, M.; Hisematsu, Y.; Ishii, T. *Environ. Int.* **1983**, *9*, 335.
(6) Healy, R. M.; Chen, Y.; Kourtchev, I.; O'Shea, D.; Wenger, J. C. *Environ. Sci. Technol.* **2012**, *46*, 11813.
(7) Chapman, O. L.; Heckert, D. C.; Reasoner, J. W.; Thackaberry, S. P. *J. Am. Chem. Soc.* **1966**, *88*, 5550.
(8) Hamanoue, K.; Nakayama, T.; Amijima, Y.; Ibuki, K. *Chem. Phys. Lett.* **1997**, *267*, 165.
(9) Fukuhara, K.; Kurihara, M.; Miyata, N. *J. Am. Chem. Soc.* **2001**, *123*, 8662.
(10) Plaza-Medina, E. F.; Rodríguez-Córdoba, W.; Morales-Cueto, R.; Peon, J. *J. Phys. Chem. A* **2011**, *115*, 577.
(11) Hurley, R.; Testa, A. C. *J. Am. Chem. Soc.* **1968**, *90*, 1949.
(12) Morales-Cueto, R.; Esquivelzeta-Rabell, M.; Saucedo-Zugazagoitia, J.; Peon, J. *J. Phys. Chem. A* **2007**, *111*, 552.
(13) Zugazagoitia, S. J.; Almora-Díaz, C. X.; Peon, J. *J. Phys. Chem. A* **2008**, *112*, 358.
(14) Zugazagoitia, S. J.; Collado-Fregoso, E.; Plaza-Medina, E. F.; Peon, J. *J. Phys. Chem. A* **2009**, *113*, 805.
(15) Vogt, R. A.; Reichardt, C.; Crespo-Hernández, C. E. *J. Phys. Chem. A* **2013**, *117*, 6580.
(16) Phousongphouang, P. T.; Arey, J. *J. Photochem. Photobiol., A* **2003**, *157*, 301.
(17) Reichardt, C.; Vogt, R. A.; Crespo-Hernández, C. E. *J. Chem. Phys.* **2009**, *131*, 224518.
(18) Vogt, R. A.; Reichardt, C.; Crespo-Hernández, C. E. *J. Phys. Chem. A* **2013**, *117*, 6580.
(19) Vogt, R. A.; Crespo-Hernández, C. E. *J. Phys. Chem. A* **2013**, *117*, 14100.
(20) Crespo-Hernández, C. E.; Vogt, R. A.; Sealey, B. *Mod. Chem. Appl.* **2013**, *1*, 106.
(21) Orozco-Gonzalez, Y.; Coutinho, K.; Peon, J.; Canuto, S. *J. Chem. Phys.* **2012**, *137*, 054307.
(22) Hamanoue, K.; Nakayama, T.; Kajiwara, K.; Yamanaka, S.; Ushida, K. *J. Chem. Soc. Faraday Trans.* **1992**, *88*, 3145.
(23) Acre, R.; Pino, E. F.; Valle, C.; Ágreda, J. *J. Phys. Chem. A* **2008**, *112*, 10294.
(24) Giussani, A.; Segarra-Martí, J.; Roca-Sanjuán, D.; Merchán, M. Excitation of Nucleobases from a Computational Perspective I: Reaction Paths. *Top. Curr. Chem.* **2013**, DOI: 10.1007/128_2013_501.
(25) Andersson, K.; Malmqvist, P.-Å.; Roos, B. O. *J. Chem. Phys.* **1992**, *96*, 1218.
(26) Roos, B. O.; Andersson, K.; Fülscher, M. P.; Malmqvist, P.-Å.; Serrano-Andrés, L.; Pierloot, K.; Merchán, M. *Adv. Chem. Phys.* **1996**, *93*, 219.
(27) Serrano-Andrés, L.; Merchán, M. Spectroscopy: Applications. In *Encyclopedia of Computational Chemistry*, Schleyer, P. v. R. ; Schreiner, P. R.; Schaefer III, H. F.; Jorgensen, W. L.; Thiel, W.; Glen, R. C., Eds.; Wiley: Chichester, 2004; pp 1−51.
(28) Aquilante, F.; De Vico, L.; Ferré, N.; Ghigo, G.; Malmqvist, P.−Å.; Pedersen, T.; Pitonak, M.; Reiher, M.; Roos, B. O.; Serrano-Andrés, L.; Urban, M.; Veryazov, V.; Lindh, R. *J. Comput. Chem.* **2010**, *31*, 224.
(29) Widmark, P.-O.; Malmqvist, P.-Å.; Roos, B. O. *Theor. Chem. Acc.* **1990**, *77*, 291.
(30) Pierloot, K.; Dumez, B.; Widmark, P.-O.; Roos, B. O. *Theor. Chem. Acta* **1995**, *90*, 87.
(31) González-Luque, R.; Climent, T.; González-Ramírez, I.; Merchán, M.; Serrano-Andrés, L. *J. Chem. Theory Comput.* **2010**, *6*, 2103.
(32) Merchán, M.; Serrano-Andrés, L. Ab Initio Method for Excited States. In *Computational Photochemistry*, 1st ed.; Olivucci, M., Ed.; Elsevier: Amsterdam, 2005; Vol. *16*, pp 35−91.
(33) Serrano-Andrés, L.; Merchán, M. Photostability and Photoreactivity in Biomolecules: Quantum Chemistry of Nucleic Acid Base Monomers and Dimers. In *Radiation Induced Molecular Phenomena in Nucleic Acids*, Leszczynski, J., Shukla, M., Eds.; Springer: The Netherlands, 2008; pp 435−472.
(34) Giussani, A.; Serrano-Andrés, L.; Merchán, M.; Roca-Sanjuán, D.; Garavelli, M. *J. Phys. Chem. B* **2013**, *117*, 1999.
(35) González-Ramírez, I.; Segarra-Martí, J.; Serrano-Andrés, L.; Merchán, M.; Rubio, M.; Roca-Sanjuán, D. *J. Chem. Theory Comput.* **2012**, *8*, 2769.
(36) De Vico, L.; Olivucci, M.; Lindh, R. *J. Chem. Theory Comput.* **2005**, *1*, 1029.
(37) Anglada, J. M.; Bofill, J. M. *J. Comput. Chem.* **1997**, *18*, 992.
(38) Garavelli, M. *Theor. Chem. Acc.* **2006**, *116*, 87.
(39) Garavelli, M.; Bernardi, F.; Cembran, A. Ab Initio Method for Excited States. In *Computational Photochemistry*, 1st ed.; Olivucci, M., Ed.; Elsevier: Amsterdam, 2005; Vol. *16*, pp 191−223.
(40) Giussani, A.; Merchán, M.; Roca-Sanjuán, D.; Lindh, R. *J. Chem. Theory Comput.* **2011**, *7*, 4088.
(41) Merchán, M.; Serrano-Andrés, L.; Robb, M. A.; Blancafort, L. *J. Am. .Chem. Soc.* **2005**, *127*, 1820.
(42) Giussani, A.; Pou-AméRigo, R.; Serrano-Andrés, L.; Freire-Corbacho, A.; Martínez-García, C.; Fernández, M. A. P.; Sarakha, M.; Canle, M. L.; Santaballa, J. A. *J. Phys. Chem. A* **2013**, *117*, 2125.
(43) Montero, R.; Longarte, A.; Peralta Conde, Á.; Redondo, C.; Castaño, F.; Gonzalez-Ramírez, I.; Giussani, A.; Serrano-Andrés, L.; Merchán, M. *J. Phys. Chem. A* **2009**, *113*, 13509.